

Regional Distribution of Articular Cartilage Thickness in the Elbow Joint

A 3-Dimensional Study in Elderly Humans

Satoshi Miyamura, MD, PhD, Takashi Sakai, MD, PhD, Kunihiro Oka, MD, PhD, Shingo Abe, MD, PhD, Atsuo Shigi, MD, Hiroyuki Tanaka, MD, PhD, Shoichi Shimada, MD, PhD, Tatsuo Mae, MD, PhD, Kazuomi Sugamoto, MD, PhD, Hideki Yoshikawa, MD, PhD, and Tsuyoshi Murase, MD, PhD

Investigation performed at Osaka University Graduate School of Medicine, Suita, Japan

Background: During elbow procedures, reconstruction of the joint (including the articular cartilage) is important in order to restore elbow function; however, the regional distribution of elbow cartilage is not completely understood. The purpose of the present study was to investigate the 3-dimensional (3-D) distribution patterns of cartilage thickness of elbow bones (including the distal part of the humerus, proximal part of the ulna, and radial head) in order to elucidate the morphological relationship among them.

Methods: Two 3-D surface models were created with use of a laser scanner: (1) a cartilage-bone model based on 20 elderly cadaveric elbows exhibiting normal cartilaginous conditions and (2) a bone model that was created after dissolving the cartilage. The 2 models were superimposed, and cartilage thickness was measured as the interval distance on the articular surface. Measurements were made at categorized anatomical points of the individual bones, and 3-D distributions on the entire articular surface were analyzed. The spatial relationship among individual bones was also assessed.

Results: In the distal part of the humerus, the cartilage was thickest in the intermediate region between the capitellum and the trochlea (mean [and standard deviation], 1.27 ± 0.17 mm); in the proximal part of the ulna, it was thickest at the anterolateral edge of the coronoid (2.20 ± 0.39 mm) and the anteroproximal edge of the proximal sigmoid notch (2.49 ± 0.55 mm); and in the radial head, it was thickest at the articular zone on the rim circumference within the dish (1.10 ± 0.17 mm) and on the proximal circumference around the side (1.02 ± 0.17 mm) ($p < 0.001$ for all). These thicker cartilage regions gathered on the joint center, facing each other.

Conclusions: The present study demonstrated regional variations in elbow cartilage thickness. The combined findings in individual bones showed “cartilage gathering” at the center of the elbow joint, which we believe to be a novel anatomical finding.

Clinical Relevance: An enhanced understanding of elbow cartilage geometry will provide additional insights into elbow procedures in elderly individuals, such as hemiarthroplasties, in which anatomical contours could help to restore normal joint function and improve postoperative outcomes.

Joint anatomy reconstruction is closely associated with the functional outcomes of elbow procedures¹⁻⁶. While reestablishing radiographically visible bone dimensions has been emphasized^{5,7-12}, the contribution of articular cartilage is not well known. The functions of the articular cartilage that covers joint surfaces include absorbing mechanical

shock and transmitting the load to the underlying subchondral bone¹³⁻¹⁵; therefore, reconstructing the cartilaginous articulation to restore elbow kinematics is important. Thus, knowledge of the native cartilage morphology of the elbow joint is useful, and quantification of cartilage thickness is of clinical interest.

Disclosure: This study was supported by the Japan Agency for Medical Research and Development (project ID 15570777) and the Japan Society for the Promotion of Science KAKENHI (grant number JP 15K10442). The **Disclosure of Potential Conflicts of Interest** forms are provided with the online version of the article (<http://links.lww.com/JBJSOA/A108>).

Copyright © 2019 The Authors. Published by The Journal of Bone and Joint Surgery, Incorporated. All rights reserved. This is an open-access article distributed under the terms of the [Creative Commons Attribution-Non Commercial-No Derivatives License 4.0](https://creativecommons.org/licenses/by-nc-nd/4.0/) (CCBY-NC-ND), where it is permissible to download and share the work provided it is properly cited. The work cannot be changed in any way or used commercially without permission from the journal.

However, despite its anatomical and clinical importance, few studies have focused on the cartilage distribution of the elbow because of an inability to accurately detect cartilage regions during image analysis in addition to the complexity of cartilage morphology. Most studies have been based on 2-dimensional imaging, including magnetic resonance imaging, and have not extended to the entire articular surface¹⁶⁻²⁰. Furthermore, the regional cartilage dimensions in individual elbow bones have been investigated separately, and, to our knowledge, no study has systematically analyzed the spatial cartilage distribution pattern in a group of individual bones throughout the elbow joint. Consequently, the 3-dimensional (3-D) distribution of elbow cartilage remains unclear and there has been no direct assessment of its morphological relationship among individual bones.

We focused on the anatomical aspects of the elbow joint and hypothesized that there would be regional variations in cartilage thickness in the elbow joint. We constructed 3-D cartilage models from cadaveric elbows of elderly donors to investigate the cartilage distribution patterns of individual elbow bones (including the distal part of the humerus, proximal part of the ulna, and radial head) in order to elucidate the morphological relationships among them. Our findings may be beneficial for joint anatomy reconstruction to restore elbow function in elderly individuals.

Materials and Methods

This cadaveric study was conducted in accordance with the tenets of the Declaration of Helsinki and received approval

from the institutional review board. All specimens were obtained from those who had agreed to be donors. Following in situ computed tomography scanning, 29 elbows from 15 formalin-embalmed cadavers were dissected to expose the articular cartilage surface of the distal part of the humerus, proximal part of the ulna, and radial head. One elbow that had malunited after a fracture and 8 degenerative elbows (defined as those with osteophytes and damage to the articular cartilage surface) were excluded on the basis of visual and radiographic inspection. The remaining 20 elbows (obtained from 6 male and 6 female donors who had had a mean age of 86.2 years [range, 74 to 95 years] at time of death) were included. Four steel spheres were firmly glued to the cortical surface at the distal or proximal third of each bone to serve as landmarks for integrating each digitized data set and surface registration²¹⁻²⁴.

Cartilage-Bone Model

Specimens were scanned with use of a 3-D optical laser scanner (Rexcan CS+ 5.0 Mega pixels; Medit) with an accuracy of $\pm 20 \mu\text{m}$ to obtain elbow joint dimensions. Scans were processed with use of ezScan7 software (Medit), and 3-D cartilage-bone models were created (Fig. 1-A).

Bone Model

To obtain baseline data for measurements of cartilage, the cartilage dissolution technique was used to create bone models without cartilage²⁵⁻³². The joint surfaces of the specimens were soaked in 6.0% sodium hypochlorite for 12 to 24 hours to

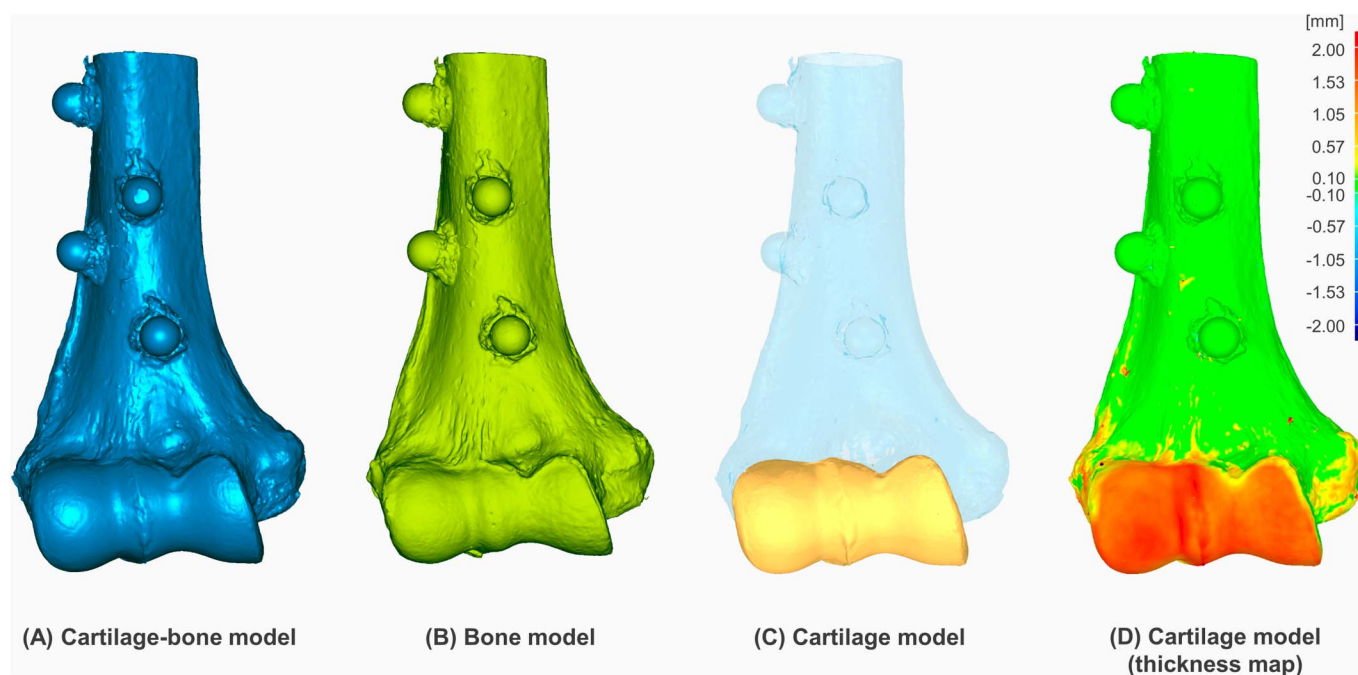


Fig. 1
Diagrams of 3-D models, including a cartilage-bone model (Fig. 1-A), a bone model (Fig. 1-B), a cartilage model (Fig. 1-C), and a cartilage model with the cartilage thickness information coded as a thickness map (Fig. 1-D).

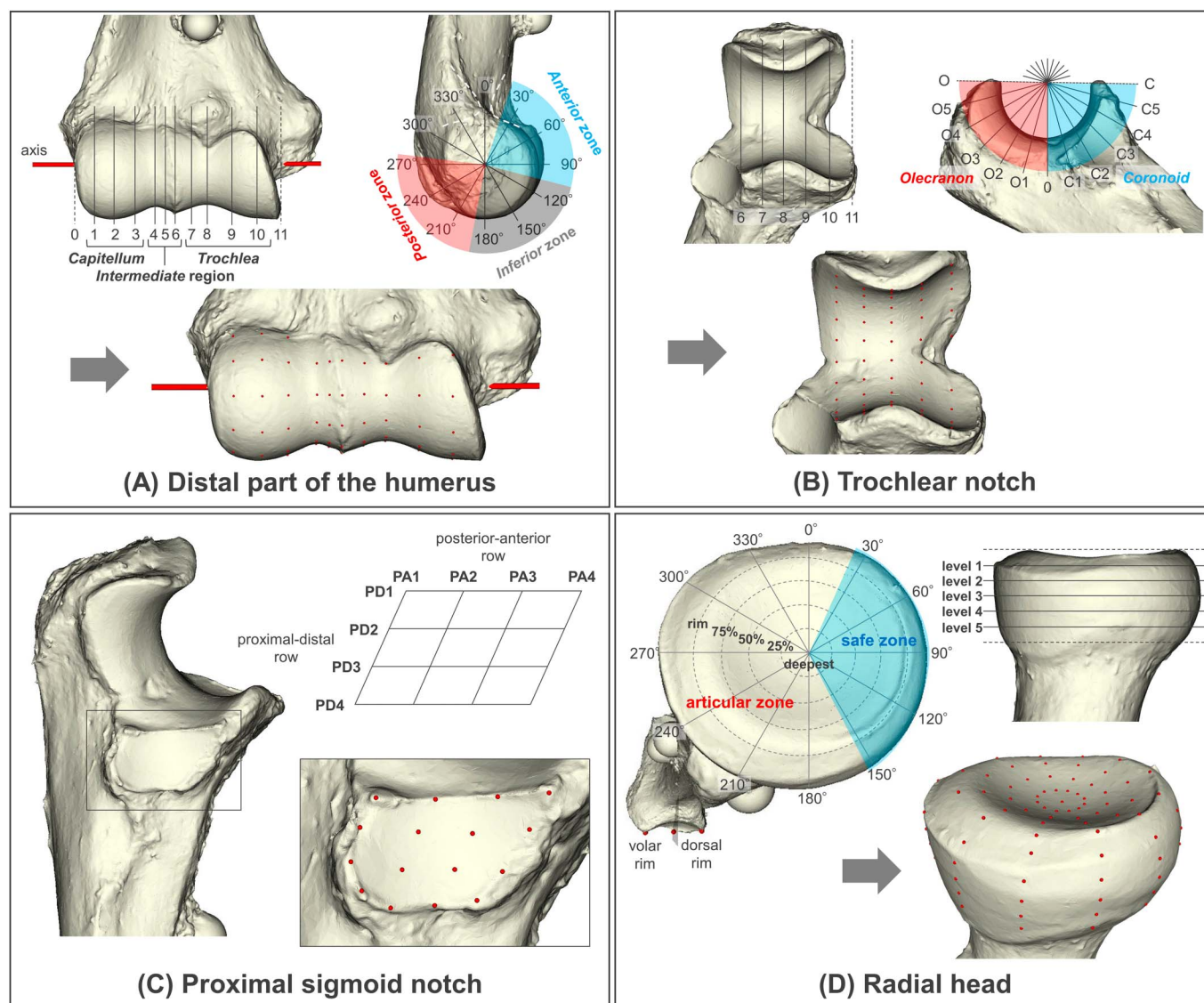


Fig. 2

Figs. 2-A through 2-D Illustrations depicting points of interest—that is, points at the intersection of the planes on the articular surface (see Appendix 1 for details). **Fig. 2-A** Distal part of the humerus. Points of interest are categorized into the *capitellum* (planes 1 through 3), the *intermediate region* (planes 4 through 6), and the *trochlea* (planes 7 through 10) in the coronal plane and into the *anterior zone* (30° , 60° , and 90° planes), *inferior zone* (120° , 150° , and 180° planes), and *posterior zone* (210° , 240° , and 270° planes) in the sagittal plane. **Fig. 2-B** Trochlear notch of the proximal part of the ulna. Points of interest are categorized into the *coronoid* (planes C1-C5) and the *olecranon* (planes O1-O5) in the sagittal plane. **Fig. 2-C** Proximal sigmoid notch of the proximal part of the ulna. Points of interest are categorized into proximal-distal rows (PD1-PD4) and posterior-anterior rows (PA1-PA4). **Fig. 2-D** For the *dish* of the radial head, rim circumference within the articular facet is determined and its intersection points with 12 planes are set. The interval between the deepest point and the rim is quadrisectioned on each plane, and the points on the same circumference (25%, 50%, 75%, and rim circumferences) are categorized. For the *side* of the radial head, points of interest on the same circumference are categorized into level 1 to level 5 circumferences. Furthermore, the area determined by the 30° , 60° , 90° , 120° , and 150° planes is defined as the *safe zone*, and the rest of the area is defined as the *articular zone*.

dissolve the articular cartilage²⁹. We visually inspected and checked the cartilage by touching the surface with a surgical probe to ensure that the cartilage was completely dissolved³¹. Then, cartilage-free bones were rescanned with use of the same procedure, and 3-D bone models were created without cartilage (Fig. 1-B).

Cartilage Model

Surface model data sets that were obtained with a 3-D laser scanner were analyzed with use of Geomagic Control software (3D Systems) in STL file format. Bone models were superimposed onto the cartilage-bone models to create a 3-D cartilage model with reference to the steel ball registration using

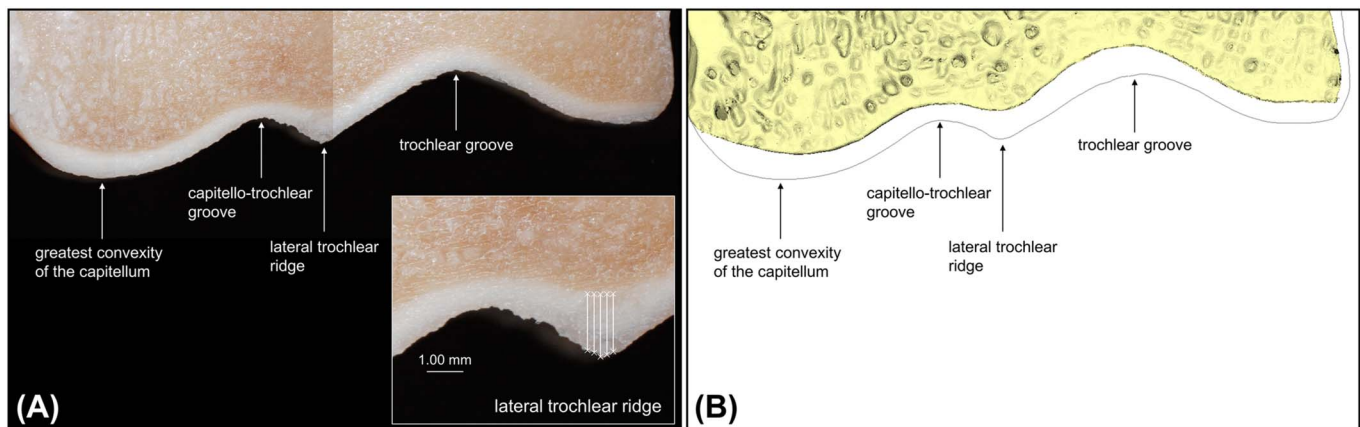


Fig. 3

Figs. 3-A and 3-B Cross-sections of the distal part of the humerus. **Fig. 3-A** Anatomical cartilage thickness of the distal part of the humerus as viewed with a stereomicroscope. Cartilage thickness was measured from the cartilage surface to the chondro-osseous junction with use of a digital template. Data were taken as the average of 5 measurements at the anatomical landmarks. **Fig. 3-B** Counterpart section of the computed models. (Additional details can be found in Appendix 2).

the iterative closest point algorithm³³, encoding the thickness information on the cartilage-bone model as a thickness map (Figs. 1-C and 1-D).

Points of Interest

STL data from the cartilage-bone model were imported into Bone Simulator software (Orthree) to define points of interest. On the articular surfaces of individual bones, points at the intersections of planes were set as points of interest based on anatomical landmarks and were saved in STL file format. All definitions and measurements were performed on the right elbow by mirroring the left side, assuming that the elbow joints on both sides are similar in anatomical configuration^{16-18,34} (Fig. 2; Appendix 1).

In the distal part of the humerus, intersection points were categorized as *capitellum*, *intermediate* region, and *trochlea* in the coronal plane. Each category was subdivided further into *anterior*, *inferior*, and *posterior* zones in the sagittal plane (Fig. 2-A).

The proximal part of the ulna was divided into trochlear and proximal sigmoid notches, and points of interest were set for each. Points of the trochlear notch were categorized as *coronoid* and *olecranon* in the sagittal plane (Fig. 2-B). On the articular surface of the proximal sigmoid notch, proximal-distal and posterior-anterior rows were categorized as PD1-PD4 and PA1-PA4, respectively (Fig. 2-C).

In the radial head, points of interest were defined as previously described by Yeung et al.³⁵, with some modifications. The articular surface of the radial head was divided into the articular facet, consisting of the radiocapitellar joint (*dish*), and the peripheral part, consisting of the proximal radioulnar joint (*side*). The deepest point of the concavity on the *dish* articular surface was identified and points on the surface of the *dish* were categorized according to their position relative to the rim of the *dish* (25% circumference, 50% circumference, 75% circumference, and rim circumference). The safe zone corresponded

to the area that did not articulate with the proximal sigmoid notch^{10,36,37}, and the rest of the area was defined as the articular zone. Around the *side* of the radial head, points along the circumference were categorized according to their position relative to the surface of the *dish* (level 1, 2, 3, 4, and 5) (Fig. 2-D).

Evaluation of Cartilage Thickness

STL data for points of interest were imported into Geomagic Control software, and cartilage thickness values were measured at each point of interest on the cartilage surface by determining the spatial minimum distance between the cartilage-bone and bone models. A grouped cartilage thickness value was calculated by averaging the values of all points of interest in a categorized region. Measurement in the computed method was validated with use of 6 samples by comparing with the stereomicroscopic findings at 4 anatomical landmarks (Fig. 3). The mean error of measurement (and standard deviation) between computational and microscopic measurements was 0.024 ± 0.017 mm (mean percentage change, $1.80\% \pm 1.65\%$) (Appendix 2).

Statistical Analysis

SPSS (version 23.0; IBM) was used to perform the statistical analyses. The level of significance was set at $p < 0.05$. The Shapiro-Wilk parametric test was used to test normality of variables.

Cartilage thickness was compared to detect differences among groups and subgroups in the distal part of the humerus and radial head. The unpaired t test or Mann-Whitney U test, with Bonferroni adjustments for multiple comparisons, was used as appropriate. With use of these tests, the average values were compared between the safe zone and the articular zone for each radial head circumference.

In the proximal part of the ulna, we assessed lateral-medial and anterior-posterior (proximal-distal) variation in cartilage thickness in the trochlear notch as well as anterior-posterior and proximal-distal variation in cartilage thickness in the proximal sigmoid notch. Partial Pearson correlation coefficients (r) were

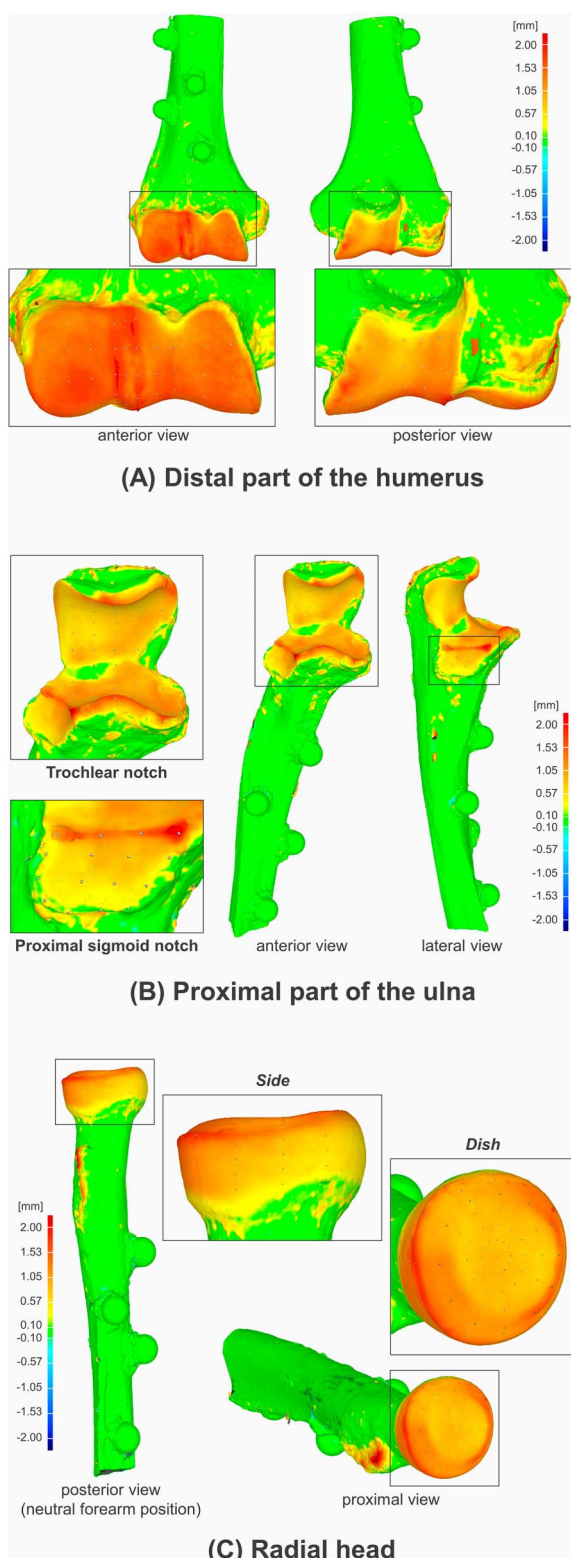


Fig. 4

Figs. 4-A, 4-B, and 4-C Cartilage distribution patterns of the individual elbow bones, represented as 3-D thickness maps from a typical subject. **Fig. 4-A** Distal part of the humerus. **Fig. 4-B** Trochlear notch and proximal sigmoid notch of the proximal part of the ulna. **Fig. 4-C** Radial head.

determined between cartilage thickness values at each point of interest and the following paired variables (planes) while controlling for other pairs: lateral-medial (planes 6 to 11) and posterior-anterior (C1-C5) in the *coronoid*, lateral-medial (planes 6 to 10) and distal-proximal (O1-O5) in the *olecranon*, and posterior-anterior (PA1-PA4) and proximal-distal (PD1-PD4) in the proximal sigmoid notch.

A priori power analyses ($\alpha = 0.05$, $\beta = 0.1$, 2-tailed) were conducted to detect a thickness difference of 0.20 ± 0.15 mm in the distal part of the humerus^{18,19,38} and radial head^{17,35,38} and to achieve $r > 0.5$ in the proximal part of the ulna. A minimum sample size of 13 specimens and 34 separate points of interest was calculated to identify meaningful differences.

Results

Three-D Cartilage Morphology in Individual Elbow Bones

The cartilage distribution patterns were represented as 3-D thickness maps from a typical subject (Fig. 4). The measurements are detailed in the tables shown in Appendix 3.

In the distal part of the humerus, the mean cartilage thickness in the *intermediate* region (1.27 ± 0.17 mm) was significantly greater than that in the *capitellum* (1.08 ± 0.14 mm; $p < 0.001$) and *trochlea* (0.96 ± 0.16 mm; $p < 0.001$). Following subdivision, the mean cartilage thickness was significantly greater in the *inferior* zone than in the *anterior* and *posterior* zones in both the *capitellum* (*anterior* zone, 1.02 ± 0.14 mm; *inferior* zone, 1.22 ± 0.18 mm; *posterior* zone, 0.65 ± 0.25 mm) (*anterior* zone versus *inferior* zone, $p < 0.001$; *inferior* zone versus *posterior* zone, $p < 0.001$) and *trochlea* (*anterior* zone, 0.91 ± 0.15 mm; *inferior* zone, 1.12 ± 0.20 mm; *posterior* zone, 0.82 ± 0.16 mm) (*anterior* zone versus *inferior* zone, $p = 0.006$; *inferior* zone versus *posterior* zone, $p < 0.01$). In the *intermediate* region, cartilage in the *anterior* zone and *inferior* zone showed similar values and was significantly thicker than that in the *posterior* zone (*anterior* zone, 1.34 ± 0.16 mm; *inferior* zone, 1.40 ± 0.24 mm; *posterior* zone, 1.06 ± 0.18 mm) (*anterior* zone versus *posterior* zone, $p < 0.001$; *inferior* zone versus *posterior* zone, $p < 0.001$) (Fig. 5).

In the proximal part of the ulna, the mean thickness values in the *coronoid*, *olecranon*, and proximal sigmoid notch were 1.04 ± 0.51 , 0.78 ± 0.30 , and 0.92 ± 0.67 mm, respectively. The trochlear notch had a small area with thinner cartilage, known as the “bare area” (0.27 ± 0.14 mm). In the *coronoid* of the trochlear notch, cartilage thickness increased as it moved laterally ($r = -0.45$; $p < 0.001$) and anteriorly ($r = 0.39$; $p < 0.001$), with a peak at the anterolateral edge (2.20 ± 0.39 mm). Conversely, cartilage was evenly distributed on the articular surface in the *olecranon* (Fig. 6-A). In the proximal sigmoid notch, cartilage thickness increased as it moved anteriorly ($r = 0.64$; $p < 0.001$) and proximally ($r = -0.73$; $p < 0.001$), with a peak at the anteroproximal edge (2.49 ± 0.55 mm) (Fig. 6-B).

Within the *dish* of the radial head, the cartilage thickness of the rim circumference (1.10 ± 0.17 mm) was significantly greater than that at all of the inner circumferences (deepest, 0.73 ± 0.15 mm; 25%, 0.73 ± 0.16 mm; 50%, 0.77 ± 0.14 mm; 75%, 0.86 ± 0.14 mm) ($p < 0.001$ for all) (Fig. 7-A). The

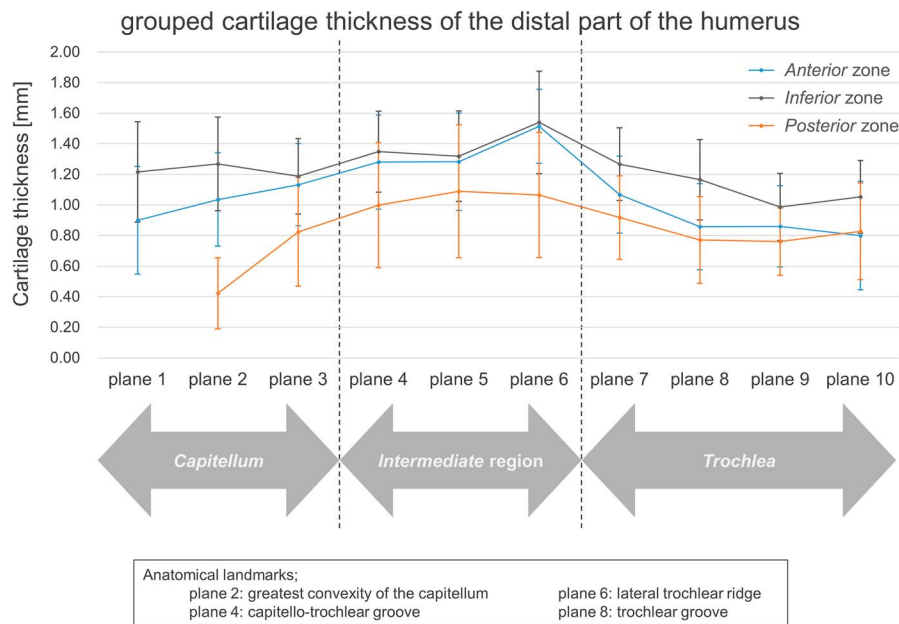


Fig. 5 Measurements and analyses in the distal part of the humerus. Abscissa = sagittal planes 1 through 10, ordinate = cartilage thickness (mm). Error bars = standard deviation.

cartilage thickness values in the articular zone were higher than those in the safe zone at the 75% circumference ($p < 0.01$) and tended to be higher at the rim circumference (Fig. 8-A). Around the *side* of the radial head, the cartilage thickness values consecutively decreased and were significantly different from level 1 to level 5 (level 1, 1.02 ± 0.17 mm; level 2, 0.71 ± 0.15 mm; level 3, 0.52 ± 0.11 mm; level 4, 0.42 ± 0.09 mm; level 5, 0.28 ± 0.07 mm) ($p < 0.001$ for all) (Fig. 7-B). The articular

zone cartilage was significantly thicker than the safe zone cartilage at all levels ($p < 0.001$ for all) (Fig. 8-B).

Morphology of the Cartilage Distribution Pattern throughout the Elbow Joint

The thicker cartilage regions in individual bones gathered at the center of the elbow joint, facing each other. The thicker areas in the distal part of the humerus (*intermediate region*) were faced

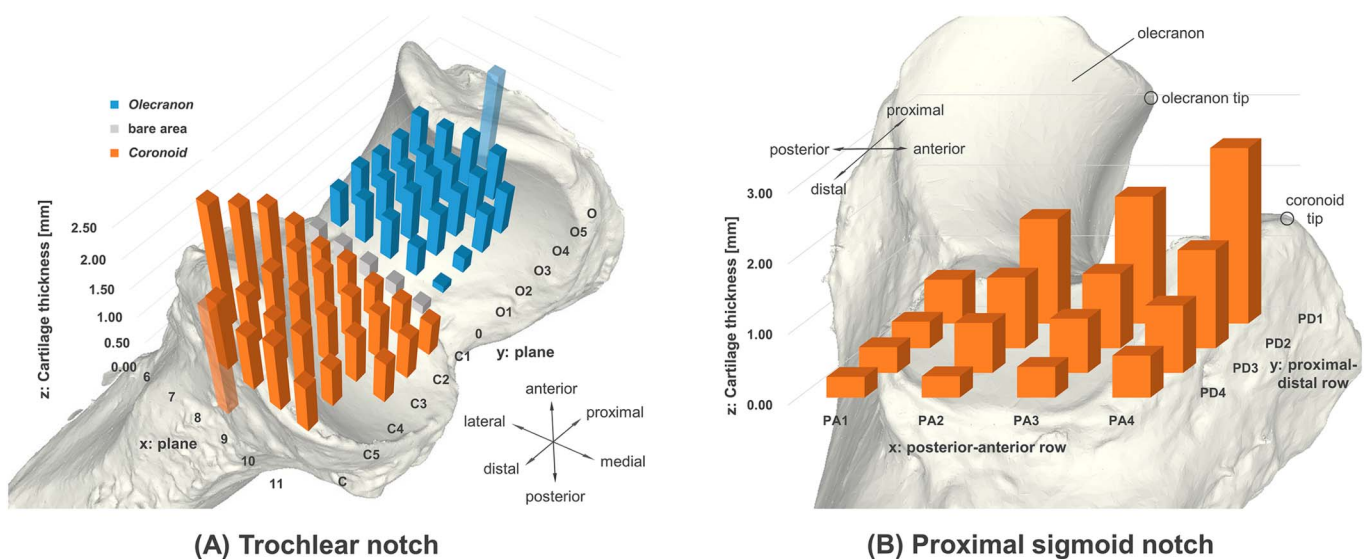


Fig. 6 **Figs. 6-A and 6-B** 3-D bar chart of the proximal part of the ulna. **Fig. 6-A** Trochlear notch. X axis = planes 6 through 11, y axis = planes C1-C5 and O1-O5, and z axis = cartilage thickness (mm). Orange bars = *coronoid* (transparent orange bar = coronoid tip), blue bars = *olecranon* (transparent blue bar = olecranon tip), and gray bars = bare area. **Fig. 6-B** Proximal sigmoid notch. X axis = posterior-anterior row, y axis = proximal-distal row, and z axis = cartilage thickness (mm).

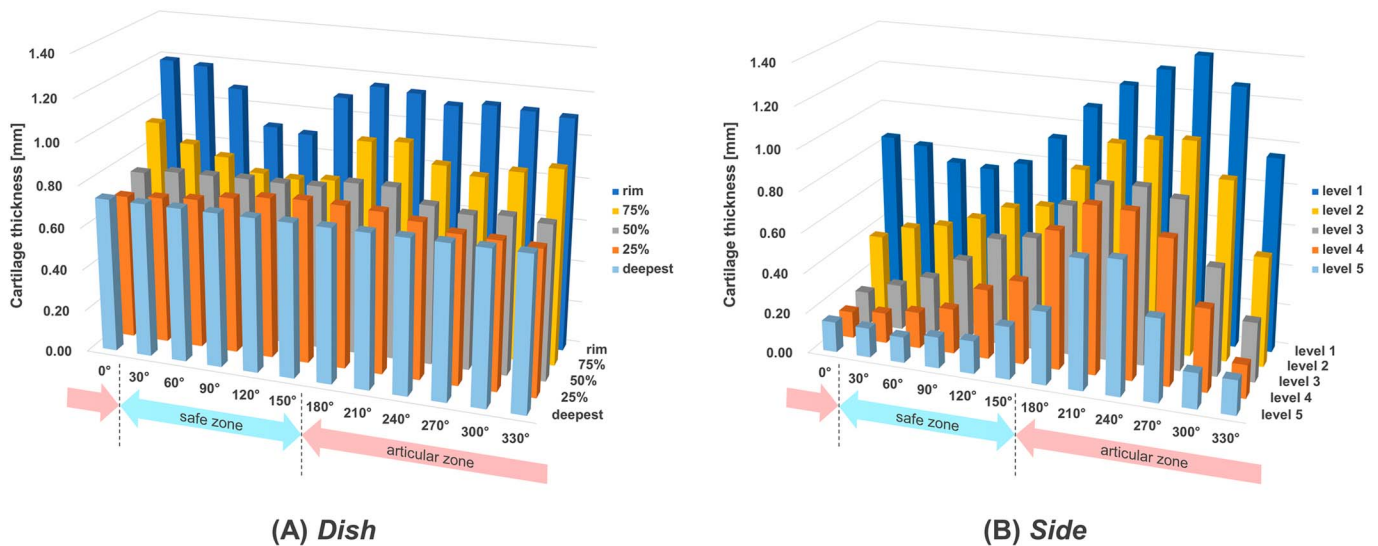


Fig. 7
Figs. 7-A and 7-B 3-D bar charts of the radial head. **Fig. 7-A Dish.** X axis = 0° to 330° planes, y axis = circumferences, and z axis = cartilage thickness (mm). Light blue bars = deepest point, orange bars = 25% circumference, gray bars = 50% circumference, yellow bars = 75% circumference, and dark blue bars = rim circumference. **Fig. 7-B Side.** X axis = 0° to 330° planes; y axis = circumferences; and z axis = cartilage thickness (mm). Light blue bars = level-1 circumference, orange bars = level-2 circumference, gray bars = level-3 circumference, yellow bars = level-4 circumference, and dark blue bars = level-5 circumference.

with the counterpart in the ulnar trochlear notch (anterolateral edge of the *coronoid*), where the ulnotrochlear joint articulates, and were also faced with the articular zone on the rim circumference within the *dish* of the radial head, where the radiocapitellar joint articulates. The thicker cartilage areas in the anteroproximal edge of the proximal sigmoid notch and in the articular zone on proximal circumferences around the *side* of the radial head faced each other at the point where the proximal radioulnar joint articulates (Figs. 9 and 10).

Discussion

Using a laser scanner, we created cartilage models from cadaveric elbows and quantified the distribution of car-

tilage thickness throughout the elbow. We found that thicker cartilage areas in individual elbow bones gathered at the joint center, facing each other. The combined findings revealed that the thicker cartilage regions were associated with articulation of the 3 joints of the elbow (Fig. 10).

First, regarding the radiocapitellar joint, our findings showed that the cartilage thickness on the rim circumference within the *dish* of the radial head was significantly greater than that on all of the inner circumferences, similar to the results reported by Yeung et al.³⁵. The articular zone cartilage was thicker than the safe zone cartilage in the outer circumferences and, facing this area, the cartilage in the *intermediate* region of the distal part of the humerus was thicker as well. These findings

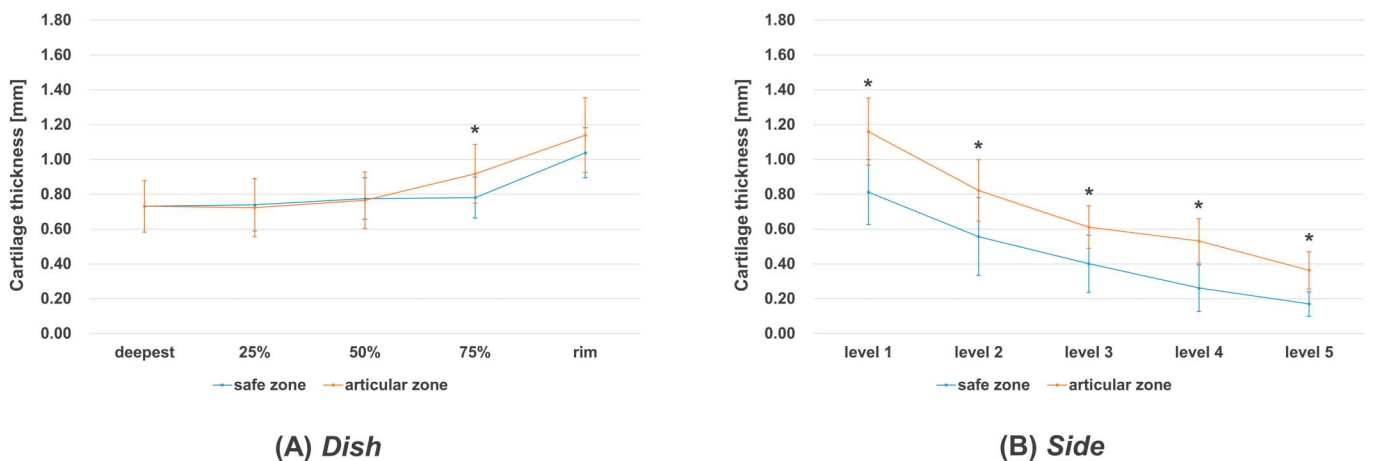


Fig. 8
Figs. 8-A and 8-B Line graphs comparing the safe zone and the articular zone in the *dish* (**Fig. 8-A**) and *side* (**Fig. 8-B**) of the radial head. Abscissa = circumferences, and ordinate = cartilage thickness (mm). Error bars = standard deviation. *p < 0.05.

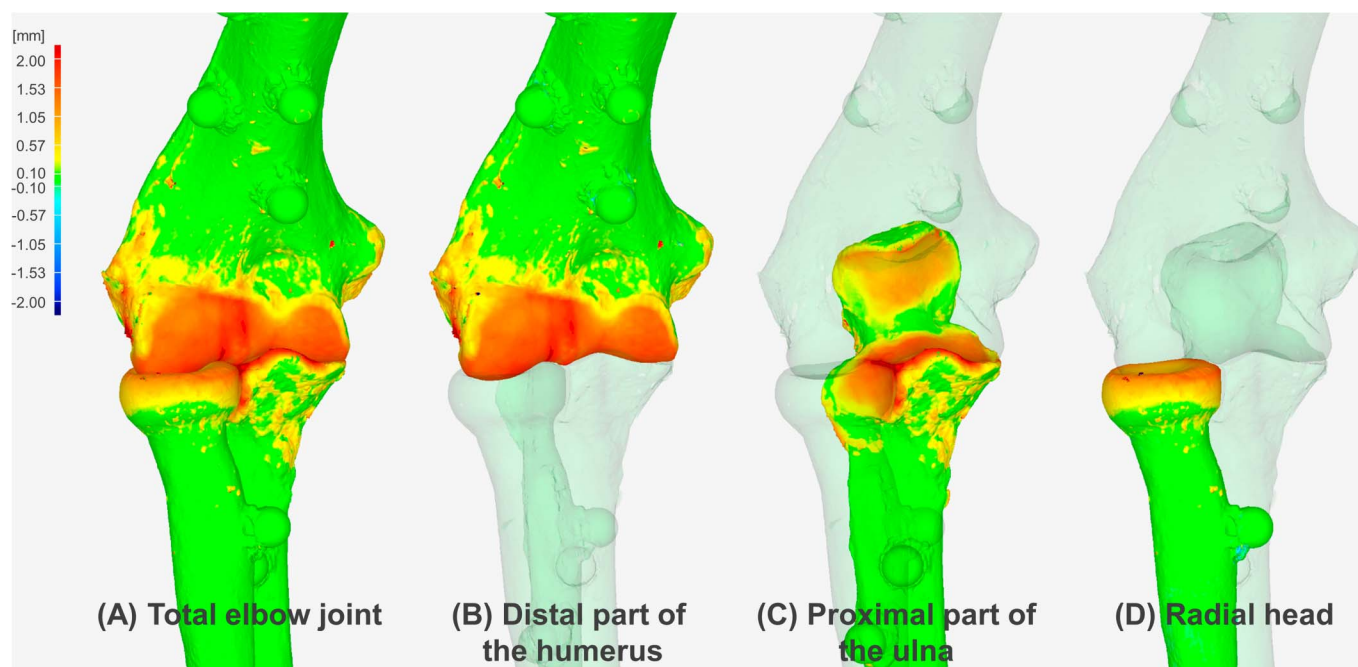


Fig. 9

Figs. 9-A through 9-D 3-D cartilage distribution pattern as a group of individual elbow bones. **Fig. 9-A** Total elbow joint. **Fig. 9-B** Distal part of humerus with transparent ulna and radius. **Fig. 9-C** Proximal part of the ulna with transparent radius and humerus. **Fig. 9-D** Radial head with transparent humerus and ulna.

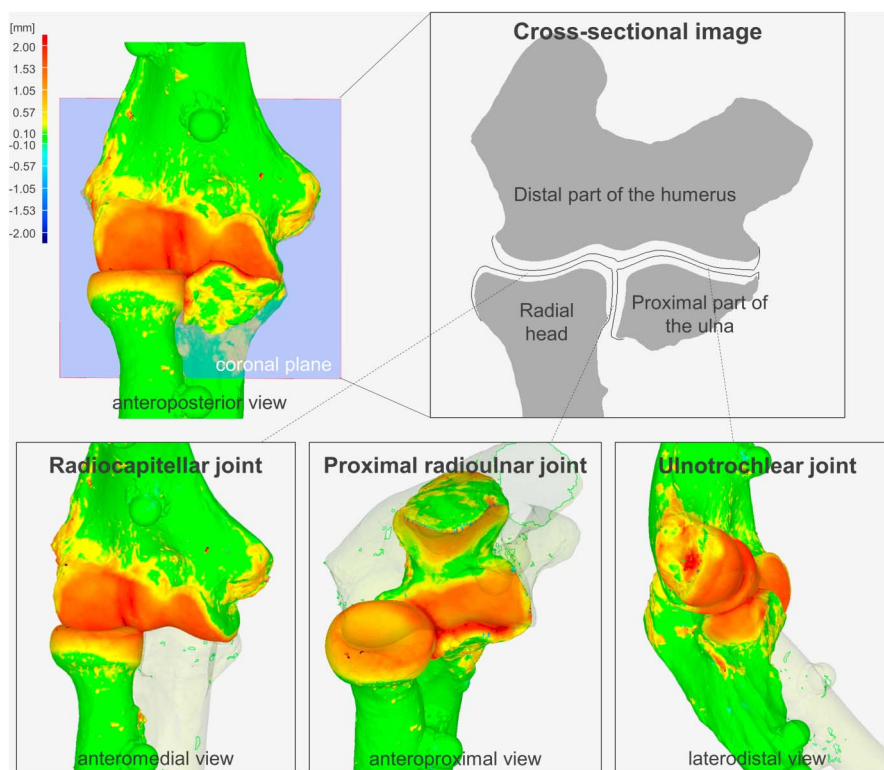


Fig. 10

Cross-sectional image and 3-D cartilage models of the 3 principal articulations: the radiocapitellar joint with transparent ulna (bottom left), the proximal radioulnar joint with transparent humerus (bottom middle), and the ulnotrochlear joint with transparent radius (bottom right). The cross-sectional image (top right) is obtained by sectioning in the coronal plane (blue).

indicated that thicker cartilage along the rim may help to increase radiocapitellar stability secondary to concavity compression onto the concave articular dish^{1,35,39-41}. Second, thicker cartilage in the ulnotrochlear joint was distributed from the anterolateral edge of the *coronoid* to the anteroproximal edge of the proximal sigmoid notch and faced the *intermediate* region of the distal part of the humerus. This asymmetrically distributed pattern was in line with the knowledge that the ulnotrochlear joint is an asymmetrical trochoid joint having an obliquity to the axis of rotation⁴². Third, in the proximal radioulnar joint, there was a thicker cartilage area in the anteroproximal edge of the proximal sigmoid notch, which was faced by the articular zone cartilage on the proximal circumferences around the *side*.

Taken together, our findings indicated that the thicker cartilage regions in individual bones gathered at the joint center. We believe that this spatial “cartilage gathering” is a novel anatomical finding, which led us to speculate that the cartilage might thicken in the area where individual bones gather, as if to fill the joint gap to fit the complex structures and stabilize the joint^{43,44}. In terms of flexion-extension motion, articulation reportedly contributes more to elbow stability in the flexed position⁴². Our results showed that cartilage thickens in the *anterior* zone of the distal part of the humerus and in the *coronoid* of the trochlear notch, where the closest relationship of the cartilage surfaces during elbow flexion provides a certain degree of joint stability⁴⁵⁻⁴⁸. These trends should be constant in this age range as long as normal cartilaginous conditions exist.

Our findings are clinically relevant to anatomical implant and prosthesis designs. Considering the spatial variability of cartilage in implant design can replicate normal human articular surface anatomy, thus restoring joint kinematics, maximizing contact area with the native articular surfaces, and potentially leading to improved postoperative outcomes^{35,49}. Several studies have experimentally revealed that subtle change in prosthetic configuration affects joint biomechanics^{1,39-41}; thus, small differences in cartilage thickness would be clinically meaningful. This concept is applicable to radial head replacement, distal humeral hemiarthroplasty, and capitellar arthroplasty in several clinical scenarios, including severe fractures, isolated degeneration at the radiocapitellar joint, and osteonecrosis⁵. Next, anatomical knowledge of cartilage thickness is useful for treating fractures. Regarding the development of arthritis, joints are believed not to tolerate step-offs of more than the cartilage thickness⁵⁰⁻⁵³; therefore, fractures occurring in thinner cartilage regions may be more susceptible to post-traumatic arthritis, potentially lowering the threshold for surgical treatment compared to fractures in regions with thicker cartilage.


Furthermore, an understanding of the spatial cartilage anatomy may help to elucidate elbow osteoarthritis. Unpredictable incongruity resulting from articular roughness with joint instability is assumed to contribute to osteoarthritic progression⁵⁴; nevertheless, there is a paucity of literature that supports these theories. Our results not only provide important information to predict the articular roughness such as post-traumatic step-offs and surface irregularities associated with

degenerative conditions but also provide a possible explanation regarding joint instability^{42,45-48}.

The present study had some limitations. First, we used formalin-embalmed cadavers. Formalin fixation can lead to dehydration of the cartilage; however, several researchers have reported that formalin fixation has no measurable effects on cartilage thickness or on geometric configuration within a joint^{21,23,25,31,55,56}. Furthermore, our measurements corresponded with those in previous *in vivo* cartilage studies¹⁶⁻¹⁹. Second, a true difference may have been overlooked due to the relatively small sample size and the study design assuming a large effect size. Also, the subjects were sampled without considering potential differences in age and sex.

In conclusion, we identified regional variations in cartilage thickness of the distal part of the humerus, proximal part of the ulna, and radial head in the elderly. Additionally, we found that thicker cartilage of individual bones gathered at the elbow joint center (“cartilage gathering”), which we believe to be a novel anatomical finding. Our findings provide additional insight that is invaluable for elbow surgery to restore normal function.

Appendix

 Supporting material provided by the authors is posted with the online version of this article as a data supplement at [jbjs.org \(http://links.lww.com/JBJSOA/A109\)](http://links.lww.com/JBJSOA/A109). ■

Note: The authors would like to thank Ryoji Nakao and Taro Adachi for their skillful technical support and excellent contributions to this study. They would also like to acknowledge Yasunobu Nakamura for his statistical support.

Satoshi Miyamura, MD, PhD¹
Takashi Sakai, MD, PhD²
Kunihiro Oka, MD, PhD¹
Shingo Abe, MD, PhD³
Atsuo Shigi, MD⁴
Hiroyuki Tanaka, MD, PhD¹
Shoichi Shimada, MD, PhD¹
Tatsuo Mae, MD, PhD¹
Kazuomi Sugamoto, MD, PhD¹
Hideki Yoshikawa, MD, PhD¹
Tsuayoshi Murase, MD, PhD¹

¹Departments of Orthopaedic Surgery (S.M., K.O., H.T., T. Mae, H.Y., and T. Murase), Neuroscience and Cell Biology (S.S.), and Orthopaedic Biomaterial Science (K.S.), Osaka University Graduate School of Medicine, Suita, Japan

²Department of Orthopaedic Surgery, Yamaguchi University Graduate School of Medicine, Ube, Japan

³Department of Orthopaedic Surgery, Toyonaka Municipal Hospital, Toyonaka, Japan

⁴Department of Orthopaedic Surgery, Yukioka Hospital, Osaka, Japan

E-mail address for T. Murase: tmurase-osk@umin.ac.jp

ORCID iD for S. Miyamura: [0000-0002-2245-5554](https://orcid.org/0000-0002-2245-5554)

ORCID iD for T. Sakai: [0000-0001-6367-1299](https://orcid.org/0000-0001-6367-1299)

ORCID iD for K. Oka: [0000-0002-7770-4634](https://orcid.org/0000-0002-7770-4634)

ORCID iD for S. Abe: [0000-0002-1451-3064](https://orcid.org/0000-0002-1451-3064)

ORCID iD for A. Shigi: [0000-0002-4309-2318](https://orcid.org/0000-0002-4309-2318)

ORCID iD for H. Tanaka: [0000-0001-8622-7422](https://orcid.org/0000-0001-8622-7422)

ORCID iD for S. Shimada: [0000-0001-5369-1069](https://orcid.org/0000-0001-5369-1069)

ORCID iD for T. Mae: [0000-0003-4586-9423](https://orcid.org/0000-0003-4586-9423)

ORCID iD for K. Sugamoto: [0000-0002-0502-7910](https://orcid.org/0000-0002-0502-7910)

ORCID iD for H. Yoshikawa: [0000-0002-7697-8035](https://orcid.org/0000-0002-7697-8035)

ORCID iD for T. Murase: [0000-0001-5628-5891](https://orcid.org/0000-0001-5628-5891)

References

- Chanlalit C, Shukla DR, Fitzsimmons JS, An KN, O'Driscoll SW. Influence of prosthetic design on radiocapitellar concavity-compression stability. *J Shoulder Elbow Surg.* 2011 Sep;20(6):885-90. Epub 2011 Jun 11.
- Giannicola G, Scacchi M, Polimanti D, Cinotti G. Discovery elbow system: 2- to 5-year results in distal humerus fractures and posttraumatic conditions: a prospective study on 24 patients. *J Hand Surg Am.* 2014 Sep;39(9):1746-56. Epub 2014 Jul 23.
- Ring D, Jupiter JB. Fractures of the distal humerus. *Orthop Clin North Am.* 2000 Jan;31(1):103-13.
- Riseborough EJ, Radin EL. Intercondylar T fractures of the humerus in the adult. A comparison of operative and non-operative treatment in twenty-nine cases. *J Bone Joint Surg Am.* 1969 Jan;51(1):130-41.
- Sabo MT, McDonald CP, Ng J, Ferreira LM, Johnson JA, King GJ. A morphological analysis of the humeral capitellum with an interest in prosthesis design. *J Shoulder Elbow Surg.* 2011 Sep;20(6):880-4. Epub 2011 Mar 30.
- Van Riet RP, Van Glabbeek F, Neale PG, Bimmel R, Bortier H, Morrey BF, O'Driscoll SW, An KN. Anatomical considerations of the radius. *Clin Anat.* 2004 Oct;17(7):564-9.
- Desai SJ, Deluce S, Johnson JA, Ferreira LM, Leclerc AE, Athwal GS, King GJ. An anthropometric study of the distal humerus. *J Shoulder Elbow Surg.* 2014 Apr;23(4):463-9. Epub 2014 Feb 20.
- Goldfarb CA, Patterson JM, Sutter M, Krauss M, Steffen JA, Galatz L. Elbow radiographic anatomy: measurement techniques and normative data. *J Shoulder Elbow Surg.* 2012 Sep;21(9):1236-46. Epub 2012 Feb 12.
- Itamura JM, Roidis NT, Chong AK, Vaishnav S, Papadakis SA, Zalavras C. Computed tomography study of radial head morphology. *J Shoulder Elbow Surg.* 2008 Mar-Apr;17(2):347-54. Epub 2008 Jan 30.
- Kuhn S, Burkhart KJ, Schneider J, Muelbert BK, Hartmann F, Mueller LP, Rommens PM. The anatomy of the proximal radius: implications on fracture implant design. *J Shoulder Elbow Surg.* 2012 Sep;21(9):1247-54. Epub 2012 Feb 9.
- Roidis N, Stevanovic M, Martirosian A, Abbott DD, McPherson EJ, Itamura JM. A radiographic study of proximal radius anatomy with implications in radial head replacement. *J Shoulder Elbow Surg.* 2003 Jul-Aug;12(4):380-4.
- Smith GR, Hotchkiss RN. Radial head and neck fractures: anatomic guidelines for proper placement of internal fixation. *J Shoulder Elbow Surg.* 1996 Mar-Apr;5(2 Pt 1):113-7.
- Adam C, Eckstein F, Milz S, Putz R. The distribution of cartilage thickness within the joints of the lower limb of elderly individuals. *J Anat.* 1998 Aug;193(Pt 2):203-14.
- Eckstein F, Reiser M, Englmeier KH, Putz R. In vivo morphometry and functional analysis of human articular cartilage with quantitative magnetic resonance imaging—from image to data, from data to theory. *Anat Embryol (Berl).* 2001 Mar;203(3):147-73.
- Ulrich-Vinther M, Maloney MD, Schwarz EM, Rosier R, O'Keefe RJ. Articular cartilage biology. *J Am Acad Orthop Surg.* 2003 Nov-Dec;11(6):421-30.
- Giannicola G, Scacchi M, Sedati P, Gumina S. Anatomical variations of the trochlear notch angle: MRI analysis of 78 elbows. *Musculoskelet Surg.* 2016 Dec;100(Suppl 1):89-95. Epub 2016 Nov 30.
- Giannicola G, Sedati P, Polimanti D, Cinotti G, Bullitta G. Contribution of cartilage to size and shape of radial head circumference: magnetic resonance imaging analysis of 78 elbows. *J Shoulder Elbow Surg.* 2016 Jan;25(1):120-6. Epub 2015 Sep 26.
- Giannicola G, Spinello P, Scacchi M, Gumina S. Cartilage thickness of distal humerus and its relationships with bone dimensions: magnetic resonance imaging bilateral study in healthy elbows. *J Shoulder Elbow Surg.* 2017 May;26(5):e128-36. Epub 2017 Jan 25.
- Schub DL, Frisch NC, Bachmann KR, Winalski C, Saluan PM. Mapping of cartilage depth in the knee and elbow for use in osteochondral autograft procedures. *Am J Sports Med.* 2013 Apr;41(4):903-7. Epub 2013 Feb 15.
- Vezeridis AM, Bae DS. Evaluation of knee donor and elbow recipient sites for osteochondral autologous transplantation surgery in capitellar osteochondritis dissecans. *Am J Sports Med.* 2016 Feb;44(2):511-20. Epub 2015 Dec 28.
- Akiyama K, Sakai T, Koyanagi J, Murase T, Yoshikawa H, Sugamoto K. Three-dimensional distribution of articular cartilage thickness in the elderly cadaveric acetabulum: a new method using three-dimensional digitizer and CT. *Osteoarthritis Cartilage.* 2010 Jun;18(6):795-802. Epub 2010 Mar 24.
- Akiyama K, Sakai T, Koyanagi J, Yoshikawa H, Sugamoto K. Morphological analysis of the acetabular cartilage surface in elderly subjects. *Surg Radiol Anat.* 2015 Oct;37(8):963-8. Epub 2015 Jan 22.
- Akiyama K, Sakai T, Sugimoto N, Yoshikawa H, Sugamoto K. Three-dimensional distribution of articular cartilage thickness in the elderly talus and calcaneus analyzing the subchondral bone plate density. *Osteoarthritis Cartilage.* 2012 Apr;20(4):296-304. Epub 2012 Jan 11.
- Neu CP, McGovern RD, Crisco JJ. Kinematic accuracy of three surface registration methods in a three-dimensional wrist bone study. *J Biomech Eng.* 2000 Oct;122(5):528-33.
- Bowers ME, Trinh N, Tung GA, Crisco JJ, Kimia BB, Fleming BC. Quantitative MR imaging using "LiveWire" to measure tibiofemoral articular cartilage thickness. *Osteoarthritis Cartilage.* 2008 Oct;16(10):1167-73. Epub 2008 Apr 14.
- Bullough PG, Jagannath A. The morphology of the calcification front in articular cartilage. Its significance in joint function. *J Bone Joint Surg Br.* 1983 Jan;65(1):72-8.
- Koff MF, Ugwonalu OF, Strauch RJ, Rosenwasser MP, Ateshian GA, Mow VC. Sequential wear patterns of the articular cartilage of the thumb carpometacarpal joint in osteoarthritis. *J Hand Surg Am.* 2003 Jul;28(4):597-604.
- Koo S, Gold GE, Andriacchi TP. Considerations in measuring cartilage thickness using MRI: factors influencing reproducibility and accuracy. *Osteoarthritis Cartilage.* 2005 Sep;13(9):782-9.
- Lalonde EA, Willing RD, Shannon HL, King GJ, Johnson JA. Accuracy assessment of 3D bone reconstructions using CT: an intro comparison. *Med Eng Phys.* 2015 Aug;37(8):729-38. Epub 2015 May 30.
- Millington SA, Grabner M, Wozelka R, Anderson DD, Hurwitz SR, Crandall JR. Quantification of ankle articular cartilage topography and thickness using a high resolution stereophotography system. *Osteoarthritis Cartilage.* 2007 Feb;15(2):205-11. Epub 2006 Sep 1.
- Miyamura S, Oka K, Sakai T, Tanaka H, Shiode R, Shimada S, Mae T, Sugamoto K, Yoshikawa H, Murase T. Cartilage wear patterns in severe osteoarthritis of the trapeziometacarpal joint: a quantitative analysis. *Osteoarthritis Cartilage.* 2019 Aug;27(8):1152-62. Epub 2019 Apr 5.
- Podolsky D, Mainprize J, McMillan C, Binhammer P. Comparison of third toe joint cartilage thickness to that of the finger proximal interphalangeal (PIP) joint to determine suitability for transplantation in PIP joint reconstruction. *J Hand Surg Am.* 2011 Dec;36(12):1950-8. Epub 2011 Nov 3.
- Besl P, McKay N. A method for registration of 3D shapes. *IEEE Trans Patt Anal.* 1992;14(2):239-56.
- Rafehi S, Lalonde E, Johnson M, King GJ, Athwal GS. An anatomic study of coronoid cartilage thickness with special reference to fractures. *J Shoulder Elbow Surg.* 2012 Jul;21(7):961-8. Epub 2011 Aug 31.
- Yeung C, Deluce S, Willing R, Johnson M, King GJ, Athwal GS. Regional variations in cartilage thickness of the radial head: implications for prosthesis design. *J Hand Surg Am.* 2015 Dec;40(12):2364-71.e1.
- Giannicola G, Manauzzi E, Sacchetti FM, Greco A, Bullitta G, Vestri A, Cinotti G. Anatomical variations of the proximal radius and their effects on osteosynthesis. *J Hand Surg Am.* 2012 May;37(5):1015-23. Epub 2012 Mar 28.
- Ries C, Müller M, Wegmann K, Pfau DB, Müller LP, Burkhart KJ. Is an extension of the safe zone possible without jeopardizing the proximal radioulnar joint when performing a radial head plate osteosynthesis? *J Shoulder Elbow Surg.* 2015 Oct;24(10):1627-34. Epub 2015 May 1.
- Graichen H, Springer V, Flaman T, Stammberger T, Glaser C, Englmeier KH, Reiser M, Eckstein F. Validation of high-resolution water-excitation magnetic resonance imaging for quantitative assessment of thin cartilage layers. *Osteoarthritis Cartilage.* 2000 Mar;8(2):106-14.
- Chanlalit C, Shukla DR, Fitzsimmons JS, Thoreson AR, An KN, O'Driscoll SW. Radiocapitellar stability: the effect of soft tissue integrity on bipolar versus monopolar radial head prostheses. *J Shoulder Elbow Surg.* 2011 Mar;20(2):219-25.
- Moon JG, Berglund LJ, Zachary D, An KN, O'Driscoll SW. Radiocapitellar joint stability with bipolar versus monopolar radial head prostheses. *J Shoulder Elbow Surg.* 2009 Sep-Oct;18(5):779-84. Epub 2009 May 7.
- Shukla DR, Fitzsimmons JS, An KN, O'Driscoll SW. Effect of radial head malunion on radiocapitellar stability. *J Shoulder Elbow Surg.* 2012 Jun;21(6):789-94. Epub 2012 Apr 21.
- An KN, Zobitz ME, Morrey BF. Biomechanics of the Elbow. In: Morrey BF, editor. *The elbow and its disorders.* 4th ed. Philadelphia: Elsevier Health Sciences; 2009. p 39-63.

43. Soslowky LJ, Flatow EL, LU Bigliani, Mow VC. Articular geometry of the glenohumeral joint. *Clin Orthop Relat Res.* 1992 Dec;285:181-90.
44. Zumstein V, Kraljević M, Müller-Gerbl M. Glenohumeral relationships: subchondral mineralization patterns, thickness of cartilage, and radii of curvature. *J Orthop Res.* 2013 Nov;31(11):1704-7. Epub 2013 Jul 1.
45. Eckstein F, Müller-Gerbl M, Steinlechner M, Kierse R, Putz R. Subchondral bone density in the human elbow assessed by computed tomography osteoabsorptiometry: a reflection of the loading history of the joint surfaces. *J Orthop Res.* 1995 Mar; 13(2):268-78.
46. Funakoshi T, Furushima K, Momma D, Endo K, Abe Y, Itoh Y, Fujisaki K, Tadano S, Iwasaki N. Alteration of stress distribution patterns in symptomatic valgus instability of the elbow in baseball players: a computed tomography osteoabsorptiometry study. *Am J Sports Med.* 2016 Apr;44(4):989-94. Epub 2016 Feb 1.
47. Miyamura S, Oka K, Abe S, Shigi A, Tanaka H, Sugamoto K, Yoshikawa H, Murase T. Altered bone density and stress distribution patterns in long-standing cubitus varus deformity and their effect during early osteoarthritis of the elbow. *Osteoarthritis Cartilage.* 2018 Jan;26(1):72-83. Epub 2017 Oct 14.
48. Momma D, Iwasaki N, Oizumi N, Nakatsuchi H, Funakoshi T, Kamishima T, Tadano S, Minami A. Long-term stress distribution patterns across the elbow joint in baseball players assessed by computed tomography osteoabsorptiometry. *Am J Sports Med.* 2011 Feb;39(2):336-41. Epub 2010 Nov 17.
49. Zhang Q, Shi LL, Ravella KC, Koh JL, Wang S, Liu C, Li G, Wang J. Distinct proximal humeral geometry in Chinese population and clinical relevance. *J Bone Joint Surg Am.* 2016 Dec 21;98(24):2071-81.
50. DeCoster TA, Willis MC, Marsh JL, Williams TM, Nepola JV, Dirschl DR, Hurwitz SR. Rank order analysis of tibial plafond fractures: does injury or reduction predict outcome? *Foot Ankle Int.* 1999 Jan;20(1):44-9.
51. Dirschl DR, Marsh JL, Buckwalter JA, Gelberman R, Olson SA, Brown TD, Llinias A. Articular fractures. *J Am Acad Orthop Surg.* 2004 Nov-Dec;12(6): 416-23.
52. Llinas A, McKellop HA, Marshall GJ, Sharpe F, Kirchen M, Sarmiento A. Healing and remodeling of articular incongruities in a rabbit fracture model. *J Bone Joint Surg Am.* 1993 Oct;75(10):1508-23.
53. Trumble T, Allan CH, Miyano J, Clark JM, Ott S, Jones DE, Fernicola P, Magnusson M, Tencer A. A preliminary study of joint surface changes after an intra-articular fracture: a sheep model of a tibia fracture with weight bearing after internal fixation. *J Orthop Trauma.* 2001 Jun-Jul;15(5):326-32.
54. Rettig LA, Hastings H 2nd, Feinberg JR. Primary osteoarthritis of the elbow: lack of radiographic evidence for morphologic predisposition, results of operative debridement at intermediate follow-up, and basis for a new radiographic classification system. *J Shoulder Elbow Surg.* 2008 Jan-Feb;17(1):97-105. Epub 2007 Nov 26.
55. Adam C, Eckstein F, Milz S, Schulte E, Becker C, Putz R. The distribution of cartilage thickness in the knee-joints of old-aged individuals — measurement by A-mode ultrasound. *Clin Biomech (Bristol, Avon).* 1998 Jan; 13(1):1-10.
56. Kurrat HJ, Oberländer W. The thickness of the cartilage in the hip joint. *J Anat.* 1978 May;126(Pt 1):145-55.